

Vacancy-induced hardening in Fe-Al alloys

This article has been downloaded from IOPscience. Please scroll down to see the full text article.

2013 J. Phys.: Conf. Ser. 443 012025

(<http://iopscience.iop.org/1742-6596/443/1/012025>)

View [the table of contents for this issue](#), or go to the [journal homepage](#) for more

Download details:

IP Address: 89.176.226.85

The article was downloaded on 13/06/2013 at 20:57

Please note that [terms and conditions apply](#).

Vacancy-induced hardening in Fe-Al alloys

F Lukáč¹, J Čížek¹, I Procházka¹, Y Jirásková², D Janičkovič³, W Anwand⁴ and G Brauer⁴

¹ Charles University in Prague, Faculty of Mathematics and Physics, V Holešovičkách 2, 18000 Praha 8, Czech Republic

² Institute of Physics of Materials, Academy of Science of the Czech Republic, Žitkova 513/22, Brno, 61662, Czech Republic

³ Institute of Physics, Slovak Academy of Science, Dúbravská cesta 9, 84511 Bratislava, Slovak Republic

⁴ Institut für Strahlenphysik, Helmholtz-Zentrum Dresden-Rossendorf, PO Box 510119, D-01314 Dresden, Germany

E-mail: lukac@mbbox.troja.mff.cuni.cz

Abstract. Hardness of Fe-Al alloys shows a non-trivial dependence on chemical composition and thermal treatment of samples and cannot be fully explained by consideration of intermetallic phases formed according to the equilibrium phase diagram of Fe-Al system. Hardening in Fe-Al alloys caused by quenched-in non-equilibrium vacancies was studied in this work. Non-equilibrium vacancies introduced into the alloys by quenching from 1000 °C were detected by means of positron annihilation spectroscopy. The concentration of quenched-in vacancies was found to strongly increase with increasing Al content from $\approx 10^{-5}$ at.⁻¹ in the alloy with $c_{Al} = 18$ at. % up to $\approx 10^{-1}$ at.⁻¹ in the alloy with $c_{Al} = 45$ at. %. Comparison of the vacancy concentration and the Vickers microhardness revealed that hardening is proportional to square root of concentration of quenched-in vacancies.

1. Introduction

Iron aluminides are well-known for their excellent mechanical properties, high temperature corrosion resistance and their low density when comparing to industrial steels. The Fe-rich part of the equilibrium phase diagram of Fe-Al system [1] exhibits intermetallic phase regions of B2, D0₃ phases and disordered A2 phase region. The mechanical properties of Fe-Al alloys change with Al composition and also after various heat treatments. Hardening caused by quenched-in non-equilibrium vacancies was proposed by Chang et al. [2] stating that a vacancy-like point defect acts as an obstacle for dislocation movement.

Positron annihilation spectroscopy provides unique methods capable of determination of vacancy concentration, namely positron lifetime spectroscopy (LT), employing simple trapping model, and variable energy slow positron annihilation spectroscopy (VEPAS), using positron diffusion length obtained from backdiffusion of implanted positrons. Recently, it has been demonstrated that VEPAS enables precise determination of vacancy concentration even in samples containing very high density of defects, where LT is not applicable due to saturated positron trapping [3]. In this work we employed VEPAS for determination of the concentration of quenched-in vacancies in Fe-Al alloys with various composition and examined the effect of vacancies on hardness.



2. Experimental

Fe-Al alloys with Al concentration c_{Al} falling in the range from 18 to 45 at.% were prepared by arc melting from high purity Fe (99.99%) and Al (99.99%) in Ti-gettered Ar atmosphere. Specimens were sealed in evacuated quartz ampoules and quench to the room temperature water after the one hour annealing at 1000 °C. The samples were investigated in the as-quenched state and after subsequent annealing at 520 °C for 1h.

A well annealed pure α -Fe (99.99%) specimen was used as a reference sample. LT characterization of this sample resulted in a single component spectrum with lifetime of (107 ± 1) ps testifying that virtually all positrons annihilate in the free state and the sample can be considered as a defect-free material. Detailed description of LT setup is described elsewhere [3].

VEPAS measurements were performed using magnetically guided energy variable positron beam "SPONSOR" [4] with slow positrons of energy from 30 eV to 35 keV. Energy spectra of annihilation γ rays were measured by HPGc detector having an efficiency of $\approx 30\%$ and an energy resolution of (1.06 ± 0.01) keV (FWHM at 511 keV). The Doppler broadening of annihilation profile was evaluated using the line-shape S -parameter. All S -parameters shown in this work were normalized to the bulk S -parameter $S_0 = 0.50784(5)$ measured in the well-annealed α -Fe reference sample at the positron energy of 35 keV. The dependence of the S -parameter on the positron energy E (so-called $S(E)$ curve) for each alloy was analysed using the VEFIT code [5].

The Vickers microhardness (HV) was measured by STRUERS Duramin-2 micro-tester. The load of 100 g was applied for 10 s.

3. Results and discussion

LT characterization of quenched alloys [3] revealed a strong contribution of positrons trapped at quenched-in vacancies. The concentration of vacancies increases with increasing Al content. In alloys with $c_{Al} > 25$ at.% the concentration of vacancies c_V is so high that it exceeds the saturated trapping limit ($c_{V,max,LT} \approx 2 \times 10^{-4}$ at. $^{-1}$). Therefore, vacancy concentration in alloys with $c_{Al} > 25$ at.% cannot be determined from LT measurements. However, VEPAS backdiffusion measurements enable to determine the concentration of vacancies also in the alloys with $c_{Al} > 25$ at.%. The the dependence of the S -parameter on the positron energy measured in the quenched alloys and the alloys subsequently annealed at 520 °C are plotted in Fig. 1(a) and 1(b), respectively. Smooth lines in Fig. 1 represent model curves calculated by VEFIT software [5] assuming two layered model consisting of (i) a thin oxide surface layer and (ii) a bulk Fe-Al layer. The thickness of the oxide layer obtained from fitting falls into the range of 5-40 nm. This surface layer exhibits high density of defects which is testified by a positron diffusion length of ~ 6 nm.

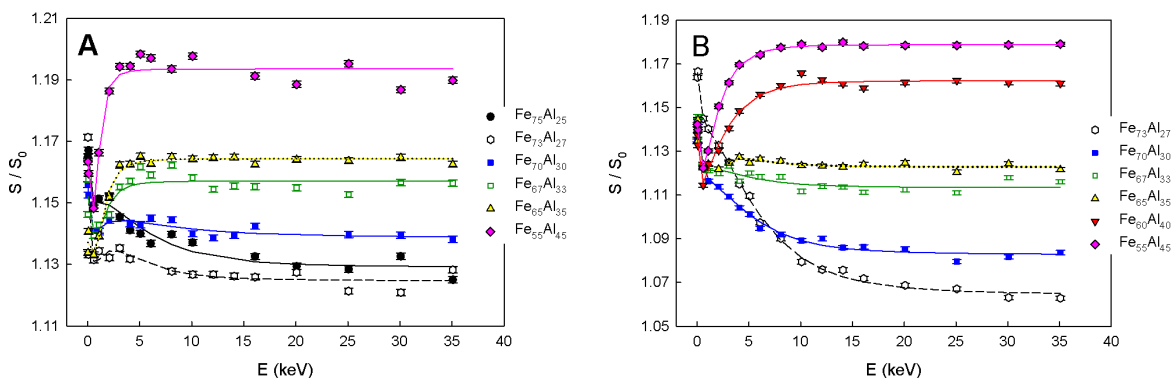


Figure 1. VEPAS results: $S(E)$ curves of various Fe-Al alloys in (a) the as-quenched state and (b) after annealing at 520 °C for 1 h.

The S-parameter and the positron diffusion length L_+ for Fe-Al bulk obtained from fitting of $S(E)$ curves are plotted in Fig. 2 for both quenched and annealed alloys. Assuming that Fe-Al alloys contain only a single type of positron traps, which was confirmed by LT spectroscopy [3], the vacancy concentration can be calculated from the formula [6]:

$$c_V = \frac{1}{\nu_V \tau_B} \left(\frac{L_{+,B}^2}{L_+^2} - 1 \right), \quad (1)$$

where $\nu_V = (4 \times 10^{14}) \text{ s}^{-1}$ is the specific positron trapping rate for Fe-vacancy [7], τ_B is the free positron lifetime in a defect-free alloys calculated theoretically in [3] and $L_{+,B}$ is the mean positron diffusion length in a defect-free alloy. This quantity can be calculated from equation

$$L_{+,B} = \sqrt{D_+ \tau_B}, \quad (2)$$

where D_+ is the room temperature positron diffusion coefficient estimated as a weighted average of positron diffusion coefficients for pure Fe and Al, i.e. $D_+ = (1 - c_{Al})D_{+,Fe} + c_{Al}D_{Al}$. The positron diffusion coefficient for aluminium $D_{+,Al} = (1.7 \pm 0.2) \text{ cm}^2\text{s}^{-1}$ was determined in [8], for iron the value $D_{+,Fe} = (1.87 \pm 0.05) \text{ cm}^2\text{s}^{-1}$ was determined using Eq. (2) from measured positron diffusion length $L_{+,Fe} = (142 \pm 2) \text{ nm}$ of well-annealed α -Fe. Bulk positron diffusion lengths $L_{+,B}$ for Fe-Al alloys estimated by Eq. 2 fall into the interval of 141-145 nm.

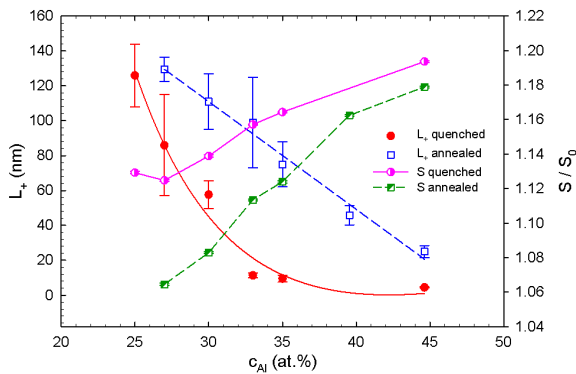


Figure 2. Positron parameters obtained from fitting of $S(E)$ curves for Fe-Al alloys: positron diffusion length L_+ and S-parameter.

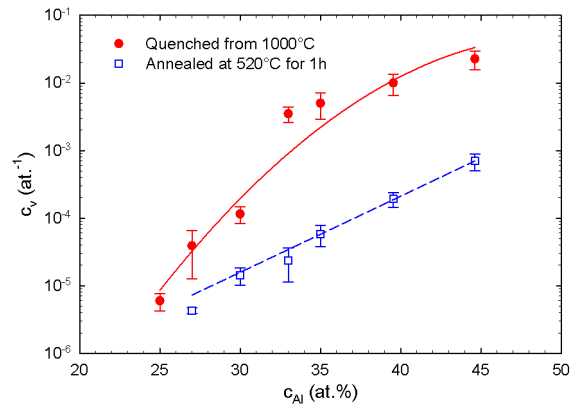


Figure 3. The vacancy concentration calculated from VEPAS results by Eq. 1.

The vacancy concentration calculated using Eq. 1 is plotted in Fig. 3 for the alloys quenched from 1000 °C and the alloys subsequently annealed at 520 °C. One can see in the figure that the concentration of quenched-in vacancies substantially increases with increasing Al content. The annealing at 520 °C leads to a significant drop of c_V indicating annihilation of vacancies.

Fig. 4 shows HV of Fe-Al alloys in the as-quenched state and after subsequent annealing at 520 °C. In alloys with $c_{Al} > 27$ at.%, the annealing at 520 °C leads to a significant drop of HV due to annihilation of vacancies. On the other hand, in alloys with $c_{Al} < 27$ at.%, the concentration of vacancies is too small to cause a detectable increase of hardness. Hence, hardness of Fe-Al alloys is a superposition of two contributions $HV = HV_V(c_V) + HV_c(c_{Al})$, where HV_V expresses hardening caused by vacancies while HV_c is the part of hardness influenced by composition. The former contribution is negligible in alloys with $c_{Al} < 27$ at.%, while in alloys with $c_{Al} > 27$ at.% both contributions are important. Since quenched-in vacancies are point obstacles pinning dislocations, $HV_V = 6\gamma\mu\sqrt{c_V}$ [2], where $\mu \sim 100 \text{ GPa}$ is the shear modulus of FeAl [9] and γ is a coefficient less than unity expressing the strength of the interaction of vacancies with a

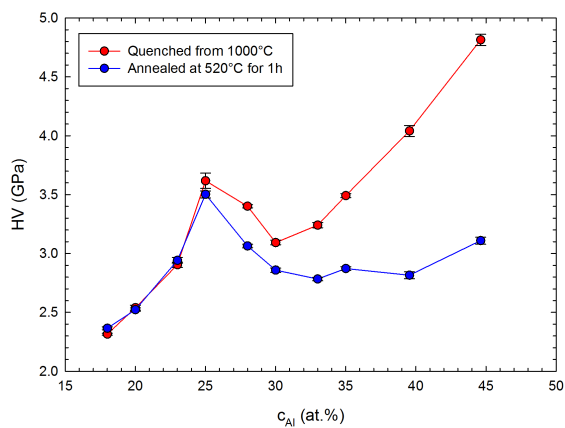


Figure 4. Microhardness of Fe-Al alloys with the Al content ranging from 18 to 45 at. %.

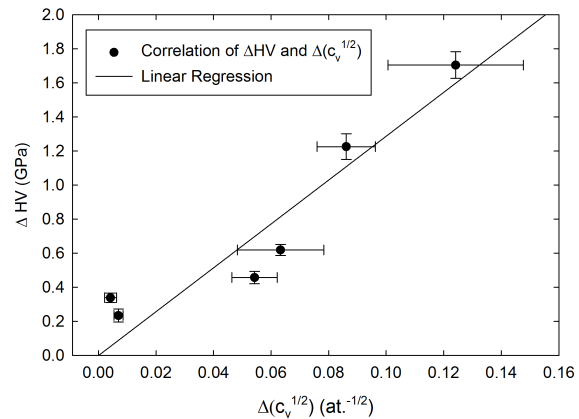


Figure 5. Difference of microhardness ΔHV between as-quenched and annealed alloy plotted as a function of the difference of $\sqrt{c_V}$.

dislocation. In order to eliminate the composition part HV_c we calculate the difference of HV between the as-quenched and the annealed sample $\Delta HV \sim \sqrt{c_{V,q}} - \sqrt{c_{V,a}}$, where $c_{V,q}$ and $c_{V,a}$ denote the concentration of vacancies in the as-quenched and the annealed state, respectively. Fig. 5 shows that ΔHV is indeed proportional to $\Delta\sqrt{c_V}$ taking into account experimental uncertainties. From the slope of this dependence we obtained $\gamma = 0.020 \pm 0.005$, which is in order of magnitude comparable with that obtained by Chang et al. [2].

4. Conclusions

The influence of quenched-in vacancies on hardness of Fe-Al alloys was investigated in the present work. It was found that the concentration of quenched-in vacancies increases with increasing Al content. Subsequent annealing at 520 °C causes a remarkable decrease of vacancy concentration. In alloys with Al content higher than 27 at.% the concentration of vacancies becomes so high that causes a significant hardening. The hardness increment in these alloys was found to be proportional to the square root of the vacancy concentration.

Acknowledgments

This work was supported by the Czech Science Foundation (Project No. P108/11/1350), Grant Agency of Charles University (Project No. 348111) and by the grant SVV-2012-265303, by the Ministry of Education, Youths and Sports of the Czech Republic (project MEB101102) and by the Deutscher Akademischer Austauschdienst DAAD (project 50755628).

References

- [1] Kubaschewski O 1982 *Iron-Binary Phase Diagrams* (Berlin: Springer-Verlag) p 5
- [2] Chang Y A, Pike L M, Liu C T, Bilbrey A R and Stone D S 1993 *Intermetallics* **1** 107
- [3] Čížek J, Lukáč F, Procházka I, Kužel R, Jirásková Y, Janičkovič D, Anwand W and Brauer G 2012 *Physica B: Condensed Matter* **407** 2659
- [4] Anwand W, Kissener H R and Brauer G 1995 *Acta Phys. Polon. A* **88** 7
- [5] Veen A, Schut H, Clement M, de Nijs J, Kruseman A and Ijpma M R 1995 *Applied Surface Science* **85** 216
- [6] Veen A, Schut H, de Vries J, Hakvoort R A and Ijpma M R 1990 *AIP Conf. Proc.* **218** 83
- [7] Schaefer H E, Damson B, Weller M, Arzt E and George E P 1997 *Physica status solidi (a)* **160** 531
- [8] Soinenen E, Huomo H, Huttunen P A, Mäkinen J, Vehanen A and Hautojärvi P 1990 *Phys. Rev. B* **41** 6227
- [9] Wolfenden A and Marmouche M 1983 *J. Metals* **35** 90